WAVE MOTION 8 (1986) 439-454
NORTH-HOLLAND

ON THE STABILITY OF WEAKLY-NONLINEAR GRAVITY-CAPILLARY WAVES

Jun ZHANG and W. K. MELVILLE

Department of Civil Engineering, Massachusetts Institute of Technology, Cambridge, MA 02139, U.S.A.

Received 1 November 1985, Revised 27 March 1986

A coupled set of equations, initially derived by Benney, is used to study the linear stability of weakly-nonlinear gravity-capillary waves to resonant triad and quartet interactions in two dimensions. The eigenvalue system is discussed for each class of resonances and certain subtleties regarding Hasselman's criterion and long wave-short wave resonances are resolved. The eigenvalue system is solved numerically and it is shown that the triad and quartet instabilities that are separated in wavenumber space for infinitesimal waves may merge for weakly nonlinear waves. Results are compared with approximations due to Benney and predictions of Zhang and Melville.

1. Introduction

Considerable advances in the study of the stability of gravity waves have been made in recent years with extensive use of numerical techniques. The general scheme, pioneered by Longuet-Higgins [1, 2], is to use numerically derived solutions for the nonlinear steady wave to calculate the matrix for the linear stability problem. The unstable modes and growth rates are then computed from the solutions to the eigenvalue problem. Subsequently, McLean et al. [3] and McLean [4] examined three-dimensional instabilities of two-dimensional gravity-wave trains. Encouraged by this work, we recently extended the numerical method to study the instabilities of deep-water gravity-capillary waves (GCW's), with results reported in Zhang and Melville [5].

In order to check the numerical scheme, we required an independent method of studying the instabilities in some range of parameter space. A search of the literature showed that a number of authors had considered the stability of weakly nonlinear GCW's but most of the published work did not contain quantitative results of sufficient detail for our purposes. This paper presents the results of our attempt to fill this gap.

Benney [6] studied the interaction between long (gravity) and short (gravity-capillary) waves in deep water, deriving a set of coupled equations which were used to examine the stability of a uniform train of GCW's. Benney's analysis showed that triad interactions (two short waves plus one long) may be significant if

$$C_{PL} \doteq C_{gs}, \tag{1.1}$$

where C_{PL} and C_{gs} are the phase and group velocity of the long and short waves, respectively. The linear growth rate of the triad instability is implied in a third-order algebraic equation (after correction of some minor errors) valid in the neighborhood of the resonance condition (1.1); however, no quantitative predictions of growth rates were presented. Djordjevic and Redekopp [7] were concerned with similar instabilities in shallow water and Benney [8] with the class of long-wave short-wave systems. Ma [9] and

Ma and Redekopp [10] studied a set of coupled equations similar to those derived in [7], but their main purpose was to consider envelope soliton solutions. In [10], it was shown that the growth rate of the triad interaction is

$$O(\varepsilon^{4/3}) \quad \text{when} \quad \left|\frac{C_{gs}-C_{PL}}{C_{gs}}\right| \leqslant O(\varepsilon^{2/3}),$$

where ε is a measure of the short-wave slope. During the course of this work, Ma [11] reported a numerical study of the instabilities of pure capillary waves in which triad interactions were not considered.

Here we follow Benney's [6] scaling and use a similar multiple-scale approach. A set of coupled equations for the surface displacement of the long and short waves and the velocity potential of the long wave is derived. These are physically equivalent to the set derived by Benney [6], which were expressed in terms of the surface displacement of the short waves and the velocity potential of the long wave. Our explicit consideration of the surface displacement of the long wave leads to a linear eigenvalue system for the stability analysis. This analysis shows that the linear growth rate and bandwidth of the triad instability for the uniform deep-water GCW train are both $O(\varepsilon/\tilde{T})$, when normalized by its frequency and wave number, respectively. (The dimensionless surface tension parameter $\tilde{T}$ is defined below.) Thus the growth rate and bandwidth are respectively slower and smaller than those found by Ma and Redekopp [10] for shallow water. As ε increases the bandwidths of the quartet and triad instabilities grow and merge.

The growth rates obtained from this weakly nonlinear theory compare very well with the strictly numerical results [5] for ε, $1/\tilde{T} \ll 1$. They are also shown to be consistent with Benney's [6] equation (3.21) when the bandwidth of the triad instability is small, but differ significantly as the bandwidth increases and the triad and quartet instabilities merge. In addition to these quantitative results, our analysis recovers Hasselman's [12] criterion which distinguishes between sum and difference resonances. Hasselman showed that a weakly nonlinear uniform wavetrain of (positive) frequency ω_0 and wave number k_0 is unstable/neutrally-stable to the sum/difference interaction described by

$$\boldsymbol{k}_1 \pm \boldsymbol{k}_2 = \boldsymbol{k}_0, \qquad \omega_1 \pm \omega_2 = \omega_0. \tag{1.2a, b}$$

Equation (1.1), the resonance condition for long-wave short-wave interaction, is just a first order approximation ($O(\tilde{T}^{-1})$) of (1.2) in the present context. However, both sum and difference interactions satisfy (1.1), in consequence of which it is only a necessary but not a sufficient condition for instability, a point that does not appear to have been explicitly considered in studies of the coupled evolution equations. We show that for ε sufficiently small, the velocity matching point (1.1) is not inside the triad instability region, and the significant disturbance components are the long wave and the lower side-band short wave.

In Section 2 we review the derivation of the coupled equations. In Section 3, these equations are used to study the instabilities of weakly nonlinear uniform GCW's. In Section 4 numerical solutions of the associated eigenvalue problem are compared with the numerical results of [5] and the predictions of [6].

2. Derivation of the coupled evolution equations

Since the purpose of this paper is to gain further insight into instabilities of gravity-capillary waves and to obtain the numerical results for checking our strictly numerical scheme, we only consider two-dimensional surface gravity-capillary waves in the deep water. The three-dimensional case may, however, be extended in a straightforward manner, with more tedious algebra.

The flow is incompressible, irrotational, and of infinite depth. The pressure on the free surface is constant and the wave slope is assumed to be small. The governing equations for the velocity potential $\phi(x, z, t)$ and the wave profile $z = \eta(x, t)$ are

$$\phi_{xx} + \phi_{zz} = 0, \quad -\infty < z < \eta(x), \tag{2.1}$$

$$\eta_t + \eta_x \phi_x - \phi_z = 0 \quad \text{on } z = \eta(x), \tag{2.2}$$

$$\phi_t + g\eta + \tfrac{1}{2}(\phi_x^2 + \phi_z^2) - \frac{T\eta_{xx}}{\rho(1+\eta_x^2)^{3/2}} = 0 \quad \text{on } z = \eta(x), \tag{2.3}$$

$$|\nabla\phi| \to 0 \quad \text{as } z \downarrow -\infty, \tag{2.4}$$

where g is the gravitational acceleration, T is the surface tension coefficient and ρ is the density. The coordinates are fixed in space with z-axis being positive upwards, and waves moving in the positive x-direction.

The derivation of the coupled long and short wave interactive equations essentially follows [6]; therefore, only the outline of this derivation is given below. A small parameter μ^2 is defined to be the ratio of the short (capillary) wave length l_c to the long (gravity) wave length l_g:

$$\mu^2 = \frac{l_c}{l_g}. \tag{2.5}$$

The nondimensional variables are indicated by primes, and given by,

$$x = l_c x', \quad z = l_c z', \quad t = t_c t', \quad \eta = \eta_c \eta', \quad \phi = \phi_c \phi' \tag{2.6}$$

$$l_c = \mu\left(\frac{T}{g\rho}\right)^{1/2}, \qquad t_c = \mu\left(\frac{l_c}{g}\right)^{1/2}, \tag{2.7}$$

$$\frac{\eta_c}{l_c} = \varepsilon, \qquad \phi_c = \frac{\varepsilon}{\mu} g^{1/2} l_c^{3/2}, \tag{2.8}$$

where ε is a small parameter, measuring the wave slope, and it is assumed that

$$\lambda\varepsilon = \mu^2, \tag{2.9}$$

where $\lambda = O(1)$.

Using equations (2.6)-(2.9), we nondimensionalize equations (2.1)-(2.4), and expand (2.2) and (2.3) on $z = 0$, dropping the primes on the dimensionless variables:

$$\phi_{xx} + \phi_{zz} = 0, \quad -\infty < z < 0, \tag{2.10}$$

$$\eta_t - \phi_z - \varepsilon\eta\phi_{zz} + \varepsilon\phi_x\eta_x - \tfrac{1}{2}\varepsilon^2\eta^2\phi_{zzz} + \varepsilon^2\eta(\phi_x\eta_x)_z = O(\varepsilon^3) \quad \text{on } z = 0, \tag{2.11}$$

$$\phi_t - \eta_{xx} + \varepsilon\eta\phi_{tz} + \lambda\varepsilon\eta + \tfrac{1}{2}\varepsilon(\phi_x^2 + \phi_z^2) + \tfrac{1}{2}\varepsilon^2\eta^2\phi_{tzz} + \tfrac{1}{2}\varepsilon^2\eta(\phi_x^2 + \phi_z^2)_z + \tfrac{3}{2}\varepsilon^2\eta_{xx}\eta_x^2 = O(\varepsilon^3) \quad \text{on } z = 0, \tag{2.12}$$

$$|\nabla\phi| \to 0 \quad \text{as } z \downarrow -\infty. \tag{2.13}$$

Equations (2.10)-(2.13) are used to derive the coupled evolution equations. In order to allow for slow modulation, we introduce the following cascade of variables:

$$\begin{aligned} &x, \quad x_1 = \varepsilon x, \quad x_2 = \varepsilon^2 x, \ldots, \\ &z, \quad z_1 = \varepsilon z, \quad z_2 = \varepsilon^2 z, \ldots, \\ &t, \quad t_1 = \varepsilon t, \quad t_2 = \varepsilon^2 t, \ldots, \end{aligned} \tag{2.14}$$

The perturbation expansions for the unknowns $\phi(x, z, t)$ and $\eta(x, t)$ are given by

$$\begin{aligned}\phi(x, z, t) = {} & \phi^{(0)}(x_1, x_2, \ldots, z_1, z_2, \ldots, t_1, t_2, \ldots) \\ & + \phi^{(1)}(x_1, x_2, \ldots, z_2, z_2, \ldots, t_1, t_2, \ldots)\, e^{i\theta} + * \\ & + \phi^{(2)}(x_1, x_2, \ldots, z_1, z_2, \ldots, t_1, t_2, \ldots)\, e^{2i\theta} + * + \cdots, \end{aligned} \tag{2.15}$$

$$\begin{aligned}\eta(x, t) = {} & \eta^{(0)}(x_1, x_2, \ldots, t_1, t_2, \ldots,) + \eta^{(1)}(x_1, x_2, \ldots, t_1, t_2, \ldots,)\, e^{i\theta} + * + \\ & \eta^{(2)}(x_1, x_2, \ldots, t_1, t_2, \ldots,)\, e^{2i\theta} + * + \cdots, \end{aligned} \tag{2.16}$$

where

$$\theta = kx - \omega t, \tag{2.17}$$

is the phase of the short wave, and * represents the complex conjugate of the preceding term; $\phi^{(0)}$, $\eta^{(0)}$ stand for the long wave potential and amplitude, respectively, and are real; $\phi^{(1)}$, $\eta^{(1)}$, $\phi^{(2)}$, $\eta^{(2)}$, ... represent the short wave potential, amplitude and their higher harmonics. The wave number and frequency of the short wave are given by k and ω, respectively. Let

$$\phi^{(0)} = \sum_{m=1}^{\infty} \varepsilon^{m-1}\phi^{(m0)}, \qquad \phi^{(n)} = \sum_{m=1}^{\infty} \varepsilon^{m-1}\phi^{(mn)} \quad \text{for } n = 1, 2, \ldots, \tag{2.18a,b}$$

$$\eta^{(0)} = \sum_{m=1}^{\infty} \varepsilon^{m-1}\eta^{(m0)}, \qquad \eta^{(n)} = \sum_{m=1}^{\infty} \varepsilon^{m-1}\eta^{(mn)} \quad \text{for } n = 1, 2, \ldots, \tag{2.18c,d}$$

Using eqs. (2.14)-(2.18), the governing equations may be reduced to a hierarchy of equations according to the order of ε and the phase function $e^{in\theta}$.

We may solve the equations step by step in increasing order of ε, and finally obtain the coupled set of equations,

$$\eta^{(0)}_{t_1} - \phi^{(0)}_{z_1} = -2\varepsilon\frac{\omega}{k}(BB^*)_{x_1} + O(\varepsilon^2), \tag{2.19a}$$

$$\phi^{(0)}_{t_1} + \lambda\eta^{(0)} = \varepsilon\eta^{(0)}_{x_1x_1} + O(\varepsilon^2), \tag{2.19b}$$

$$\nabla^2\phi^{(0)} = O(\varepsilon^2), \qquad \phi^{(0)}_{z_1} \to 0 \quad \text{as } z_1 \to -\infty, \tag{2.19c}$$

$$B_{t_1} + \frac{3}{2}\frac{\omega}{k}\left(1 - \frac{\varepsilon\lambda}{6k^2}\right)B_{x_1} = \varepsilon\left\{\frac{3ik}{8\omega}B_{x_1x_1} + \frac{1}{4}ik\omega B^2B^* - B\omega\left[\frac{3}{2}\eta^{(0)}_{x_1} + \frac{ik}{\omega}\phi^{(0)}_{x_1} + \frac{k}{\omega}\eta^{(0)}_{t_1}\right]\right\} + O(\varepsilon^2), \tag{2.19d}$$

where

$$B = A\exp(i\lambda x_1\theta/3k), \tag{2.20}$$

and A is defined by

$$\eta^{(1)} = \frac{i\omega}{k^2}A + \varepsilon\left\{\frac{1}{k^2}\frac{\partial}{\partial t_1} + \frac{1}{\omega}\frac{\partial}{\partial x_1} + \frac{i\omega}{k}\eta^{(0)}\right\}A + O(\varepsilon^2). \tag{2.21}$$

Therefore, B is proportional to the amplitude of the short waves.

It may be shown that (2.19a)-(2.19d) are equivalent to (3.3)-(3.5) of [6]. The reason for expressing the coupled equations in our form is to have a linear eigenvalue system in later stability analyses.

3. Stability of a uniform short-wave train

Equations (2.19a)-(2.19d) are coupled: the nonlinearity of the short wave on the right-hand side of (2.19a) forces the long waves, and (2.19d) is a standard nonlinear Schrödinger equation plus the interaction terms between the short and long waves.

A particular solution of the coupled equations is a uniform short wave train with no long waves; that is,

$$\eta^{(0)} = 0, \qquad B = S_0 \exp\{\tfrac{1}{4}\mathrm{i}k\omega|S_0|^2\varepsilon t_1\}, \tag{3.1}$$

where S_0 is a measure of the wave steepness of the uniform wave train, and is independent of x and t.

We now consider a uniform short wave train perturbed by a long wave and side-band wave disturbances:

$$\phi^{(0)} = \frac{1}{2}\frac{\omega}{k^2}\varepsilon\, \mathrm{e}^{Kz_1}(\mathrm{i}\hat{c}\mathrm{e}^{\mathrm{i}(Kx_1-\Omega t_1)} + *), \tag{3.2}$$

$$\eta^{(0)} = \frac{1}{2}\frac{\varepsilon}{k}(\hat{a}\, \mathrm{e}^{\mathrm{i}(Kx_1-\Omega t_1)} + *), \tag{3.3}$$

$$B = \frac{k}{\omega}S_0(1+\varepsilon B_1+\varepsilon B_2)\exp\{\tfrac{1}{4}\mathrm{i}\varepsilon\omega|S_0|^2 t_1\}, \tag{3.4}$$

and

$$B_1 = \hat{b}_1 \exp[\mathrm{i}(Kx_1-\Omega t_1)], \qquad B_2 = \hat{b}_2 \exp[-\mathrm{i}(Kx_1-\Omega t_1)], \tag{3.4a,b}$$

where $\eta^{(0)}$, εB_1 and εB_2 are the modulational disturbances on the short wave profile. We may interpret εB_1 as the higher side-band disturbance (with a slightly higher frequency than the uniform short wave) and εB_2 as the lower side-band disturbance (with a slightly lower frequency than the uniform short wave), respectively. The unknowns, $\hat{a}$, $\hat{c}$, $\hat{b}_1$, $\hat{b}_2$ may be complex. The long wave potential $\phi^{(0)}$ is given by (3.2) so that (2.19c) is implicitly satisfied.

Substituting the perturbations (3.2)-(3.4) into the coupled equations (2.19), we have the following four simultaneous equations:

$$\frac{\Omega}{\omega}\hat{a} + \frac{K}{k}\hat{c} = 4\varepsilon|S_0|^2\frac{K}{k}(\hat{b}_1+\hat{b}_2^*), \qquad \frac{\Omega}{\omega}\hat{c} + \frac{\lambda}{k^2}\hat{a} = -\varepsilon\hat{a}\left(\frac{K}{k}\right)^2, \tag{3.5a,b}$$

$$\frac{\Omega}{\omega}\hat{b}_1 - \frac{3}{2}\left(1-\frac{\varepsilon\lambda}{6k^2}\right)\left(\frac{K}{k}\right)\hat{b}_1 = \frac{3\varepsilon}{8}\left(\frac{K}{k}\right)^2\hat{b}_1 - \frac{\varepsilon}{4}|S_0|^2(\hat{b}_1+\hat{b}_2^*) - \frac{3\varepsilon}{4}\frac{K}{k}\hat{a}, \tag{3.5c}$$

$$\frac{\Omega}{\omega}\hat{b}_2^* - \frac{3}{2}\left(1-\frac{\varepsilon\lambda}{6k^2}\right)\left(\frac{K}{k}\right)\hat{b}_2^* = -\frac{3\varepsilon}{8}\left(\frac{K}{k}\right)^2\hat{b}_2^* + \frac{\varepsilon}{4}|S_0|^2(\hat{b}_1+\hat{b}_2^*) + \frac{3\varepsilon}{4}\frac{K}{k}\hat{a} - \varepsilon\frac{\Omega}{\omega}\hat{a}. \tag{3.5d}$$

Expressing K, Ω in terms of x, t (instead of x_1 and t_1) eq. (3.5) may be written in the matrix form

$$\frac{\Omega}{\omega}[X]\{u\} = [Y]\{u\}, \tag{3.6}$$

where

$$[X]=\begin{vmatrix} 1 & 0 & 0 & 0 \\ 0 & 1 & 0 & 0 \\ 0 & 0 & 1 & 0 \\ \varepsilon & 0 & 0 & 1 \end{vmatrix},$$

$$[Y]=\begin{vmatrix} 0 & \dfrac{-K}{k} & \varepsilon\dfrac{K}{k} & \varepsilon\dfrac{K}{k} \\ -\dfrac{1}{\tilde{T}}-\left(\dfrac{K}{k}\right)^2 & 0 & 0 & 0 \\ \dfrac{3}{4}\varepsilon\dfrac{K}{k} & 0 & \dfrac{3}{2}\left(1-\dfrac{1}{6\tilde{T}}\right)\dfrac{K}{k}+\dfrac{3}{8}\left(\dfrac{K}{k}\right)^2-\dfrac{\varepsilon^2}{16} & -\dfrac{\varepsilon^2}{16} \\ \dfrac{3}{4}\varepsilon\dfrac{K}{k} & 0 & \dfrac{\varepsilon^2}{16} & \dfrac{3}{2}\left(1-\dfrac{1}{6\tilde{T}}\right)\dfrac{K}{k}-\dfrac{3}{8}\left(\dfrac{K}{k}\right)^2+\dfrac{\varepsilon^2}{16} \end{vmatrix},$$

and $\{u\}^{\mathrm{T}}=(\hat{a}, \hat{c}, \hat{b}_1, \hat{b}_2^*)$ is the eigenvector, corresponding to the eigenvalue Ω/ω.

In deriving (3.6), the following equalities were used:

$$|S_0|^2=\tfrac{1}{4}, \tag{3.7}$$

$$\frac{\varepsilon\lambda}{k^2}=\frac{1}{\tilde{T}}, \tag{3.8}$$

where $\tilde{T}=Tk^2/\rho g$ is the nondimensional surface tension coefficient. The derivation of (3.7) and (3.8) is given in Appendix A.

Equation (3.6) is further simplified to the form

$$\frac{\Omega}{\omega}[I]\{u\}=[X]^{-1}[Y]\{u\}, \tag{3.9}$$

where $[I]$ is the unit matrix. The eigenvalue problem (3.9) may be accurately solved by EIGCC algorithm [13]. The positive imaginary part of the eigenvalues is the linear growth rate of the instability.

Before we show the numerical results we may approximate (3.9) by a simpler form in order to reveal certain characteristics of triad and quartet instabilities. Using (3.5b), the fourth-order matrix $[Y]$ may be reduced to third-order, at the cost of (3.6) no longer being linear in Ω/ω.

Then, substituting $\Omega/\omega=[\bar{\Omega}+\frac{3}{2}(1-1/6\tilde{T})]K/k$, on the left-hand side of (3.6) we have

$$\bar{\Omega}[I]\{u_1\}=[Y_1]\{u_1\}, \tag{3.10}$$

where

$$[Y_1]=\begin{vmatrix} \dfrac{(1/\tilde{T})[1+\tilde{T}(K/k)^2]}{\Omega/\omega}-\dfrac{3}{2}\left(1-\dfrac{1}{6\tilde{T}}\right) & \varepsilon & \varepsilon \\ \dfrac{3}{4}\varepsilon & \dfrac{3}{8}\left(\dfrac{K}{k}\right)-\dfrac{\varepsilon^2}{16}\dfrac{k}{K} & -\dfrac{\varepsilon^2}{16}\dfrac{k}{K} \\ \dfrac{3}{4}\varepsilon & \dfrac{\varepsilon^2}{16}\dfrac{k}{K} & -\dfrac{3}{8}\left(\dfrac{K}{k}\right)+\dfrac{\varepsilon^2}{16}\dfrac{k}{K} \end{vmatrix}, \tag{3.11}$$

and $\{u_1\}^{\mathrm{T}}=(\hat{a}, \hat{b}_1, \hat{b}_2^*)$.

Two interesting cases in which the uniform wave train is unstable are worth discussing.

Case 1.

$$\left[\frac{1}{\tilde{T}}\frac{[1+\tilde{T}(K/k)^2]}{\Omega/\omega}-\frac{3}{2}\left(1-\frac{1}{6\tilde{T}}\right)\right]\gg O(\varepsilon). \tag{3.12}$$

The above inequality may be approximately written as

$$\frac{C_{PL}-C_{gs}}{C_{PS}}\gg O(\varepsilon, 1/\tilde{T}),$$

if we notice[1]

$$\frac{1+\tilde{T}[K/k]^2}{\tilde{T}\Omega/\omega}=\frac{C_{PL}}{C_{PS}}+O(\varepsilon, 1/\tilde{T}), \tag{3.13}$$

where $C_{PL}=\Omega/k$; $C_{PS}=\omega/K$, is the phase velocity of the short wave; and

$$C_{gs}=\frac{3}{2}\frac{\omega}{k}\frac{\tilde{T}+\frac{1}{3}}{\tilde{T}+1}.$$

Equation (3.12) ensures that the long wave's phase velocity is quite different from the short wave's group velocity.

In this case, the eigenvalue system (3.11) degenerates to the following form:

$$\bar{\Omega}_1 \doteq C_{PL}/C_{gs}, \tag{3.14}$$

and

$$\frac{K}{k}\bar{\Omega}_{2,3}[I]\begin{Bmatrix}\hat{b}_1\\ \hat{b}_2^*\end{Bmatrix}=\begin{vmatrix}\frac{3}{8}\frac{K^2}{k^2}-\frac{\varepsilon^2}{16} & -\frac{\varepsilon^2}{16}\\ \frac{\varepsilon^2}{16} & -\frac{3}{8}\frac{K^2}{k^2}+\frac{\varepsilon^2}{16}\end{vmatrix}\begin{Bmatrix}\hat{b}_1\\ \hat{b}_2^*\end{Bmatrix}. \tag{3.15}$$

From (3.15), we have

$$\frac{K}{k}\bar{\Omega}_{2,3}\doteq\pm\frac{3}{8}\left[\left\{\frac{K}{k}\right\}^2-\frac{\varepsilon^2}{3}\right]. \tag{3.16}$$

The instability will occur if $0<K/k<\varepsilon/\sqrt{3}$, and the maximum growth rate of the instability is

$$I_m\frac{\Omega}{\omega}\doteq\frac{1}{16}\varepsilon^2, \tag{3.17}$$

when $K/k=\varepsilon/\sqrt{6}$.

It is not difficult to recognize that the instability shown in (3.15)-(3.17) is due to the quartet resonant interaction (or side-band instability) in the case of the pure capillary wave train with infinite depth. The same results may be obtained from Djordjevic and Redekopp [7] (eq. 2.21) and [6] (eq. 3.16).

Case 2.

$$\left[\frac{1}{\tilde{T}}\frac{[1+\tilde{T}(K/k)^2]}{\Omega/\omega}-\frac{3}{2}\left(1-\frac{1}{6\tilde{T}}\right)\right]\sim O(\varepsilon). \tag{3.18}$$

[1] See Appendix B.

As the analysis of Case 1 shows, (3.18) is satisfied near the point where (1.1) is satisfied; hence we rescale K/k near this point in order to linearize the eigenvalue system (3.10) in Ω/ω. Let

$$\frac{K}{k}=\frac{4}{9\tilde{T}}(1+\varepsilon K_r), \tag{3.19}$$

and

$$\frac{\Omega}{\omega}=\Omega_0(1+\Omega_r), \tag{3.20}$$

where

$$\Omega_0=\frac{3}{2}\left[1-\frac{1}{6\tilde{T}}\right]\frac{K}{k}. \tag{3.21}$$

It is easy to show that[2]

$$\Omega_r=O(\varepsilon, 1/\tilde{T}). \tag{3.21a}$$

Therefore, (3.11) may be linearized in Ω_r, and we have

$$\Omega_0\Omega_r[I]\{u_1\}=[Y_2]\{u_1\}, \tag{3.22}$$

where

$$[Y_2]=\begin{vmatrix} \frac{1}{3\tilde{T}}\left(\frac{43}{81}\frac{1}{\tilde{T}}-\varepsilon K_r\right) & \frac{2\varepsilon}{9\tilde{T}} & \frac{2\varepsilon}{9\tilde{T}} \\ \frac{1}{3}\frac{\varepsilon}{\tilde{T}} & \frac{2}{27}\frac{1}{\tilde{T}^2}-\frac{\varepsilon^2}{16} & -\frac{\varepsilon^2}{16} \\ -\frac{1}{3}\frac{\varepsilon}{\tilde{T}} & \frac{\varepsilon^2}{16} & -\frac{2}{27}\frac{1}{\tilde{T}^2}+\frac{\varepsilon^2}{16} \end{vmatrix}. \tag{3.23}$$

The higher order terms $O(\varepsilon/\tilde{T}^2)$, $O(\varepsilon^2/\tilde{T})$ are neglected in (3.23).

The eigenvalue system (3.22) is used to study the characteristics of the triad instability. Assume that there are only the components of long and lower side band waves in the disturbance (i.e. $b_1=0$); eq. (3.22) may be further reduced to

$$\Omega_0\Omega_r[I]\begin{Bmatrix}\hat{a}\\ \hat{b}_2^*\end{Bmatrix}=\begin{vmatrix} \frac{1}{3\tilde{T}}\left(\frac{43}{81}\frac{1}{\tilde{T}}-\varepsilon K_r\right) & \frac{2\varepsilon}{9\tilde{T}} \\ -\frac{1}{3}\frac{\varepsilon}{\tilde{T}} & -\frac{2}{27}\frac{1}{\tilde{T}^2}+\frac{\varepsilon^2}{16} \end{vmatrix}\begin{Bmatrix}\hat{a}\\ \hat{b}_2^*\end{Bmatrix}. \tag{3.24}$$

Equation (3.24) may be solved to give

$$\Omega_0\Omega_r=\frac{(\frac{25}{243}\tilde{T}^{-2}-\frac{1}{3}\varepsilon K_r\tilde{T}^{-1}+\frac{1}{16}\varepsilon^2)\pm[(\frac{61}{243}\tilde{T}^{-2}-\frac{1}{3}\varepsilon K_r\tilde{T}^{-1}-\frac{1}{16}\varepsilon^2)^2-\frac{8}{27}\varepsilon^2\tilde{T}^{-2}]^{1/2}}{2}. \tag{3.25}$$

Instability will occur when

$$\tfrac{61}{243}\tilde{T}^{-2}-\tfrac{1}{16}\varepsilon^2-\tfrac{2}{3}(\tfrac{2}{3})^{1/2}\varepsilon/\tilde{T}\leq\tfrac{1}{3}\varepsilon K_r\tilde{T}^{-1}\leq\tfrac{61}{243}\tilde{T}^{-2}-\tfrac{1}{16}\varepsilon^2+\tfrac{2}{3}(\tfrac{2}{3})^{1/2}\varepsilon/\tilde{T}$$

or

$$\tfrac{4}{9}\tilde{T}^{-1}+\tfrac{244}{729}\tilde{T}^{-2}-\tfrac{1}{12}\varepsilon^2-\tfrac{8}{9}(\tfrac{2}{3})^{1/2}\varepsilon/\tilde{T}\leq K/k\leq\tfrac{4}{9}\tilde{T}^{-1}+\tfrac{244}{729}\tilde{T}^{-2}-\tfrac{1}{12}\varepsilon^2+(\tfrac{8}{9})(\tfrac{2}{3})^{1/2}\varepsilon/\tilde{T}. \tag{3.26}$$

[2] See Appendix B.

The normalized bandwidth of the instability is

$$\Delta K/k = \tfrac{16}{9}(\tfrac{2}{3})^{1/2}\varepsilon/\tilde{T}. \tag{3.27}$$

The maximum growth rate of the triad instability is

$$\operatorname{Im}\Omega/\omega = \tfrac{1}{3}(\tfrac{2}{3})^{1/2}\varepsilon/\tilde{T}, \tag{3.28}$$

when

$$K/k = \tfrac{4}{9}\tilde{T}^{-1} + \tfrac{244}{729}\tilde{T}^{-2} - \tfrac{1}{12}\varepsilon^2. \tag{3.29}$$

We notice that (3.29) with $\varepsilon = 0$ is the approximation of the linear sum triad resonance condition (1.2) to the second order $O(1/\tilde{T}^2)$. Thus, the triad resonance interaction may occur for the 'triad' of the long, lower side-band wave disturbance and the uniform short wave.

Now we assume that there are only the components of long wavelength and higher side-band waves in the disturbances (i.e., $\hat{b}_2 = 0$). Equation (3.23) is reduced to

$$\Omega_0\Omega_r[I]\begin{Bmatrix}\hat{a}\\ \hat{b}_1\end{Bmatrix} = \begin{vmatrix} \frac{1}{3\tilde{T}}\left(\frac{43}{81}\frac{1}{\tilde{T}} - \varepsilon K_r\right) & \frac{2\varepsilon}{9\tilde{T}} \\ \frac{1}{3}\frac{\varepsilon}{\tilde{T}} & \frac{2}{27}\frac{1}{\tilde{T}^2} - \frac{\varepsilon^2}{16} \end{vmatrix} \begin{Bmatrix}\hat{a}\\ \hat{b}_1\end{Bmatrix}. \tag{3.30}$$

Solving (3.30), we have

$$\Omega_0\Omega_r = \tfrac{1}{2}\{(\tfrac{61}{243}\tilde{T}^{-2} - \tfrac{1}{3}\varepsilon K_r\tilde{T}^{-1} - \tfrac{1}{16}\varepsilon^2) \pm [(\tfrac{25}{243}\tilde{T}^{-2} - \tfrac{1}{3}\varepsilon K_r\tilde{T}^{-1} + \tfrac{1}{16}\varepsilon^2)^2 + \tfrac{8}{27}\varepsilon^2\tilde{T}^{-2}]^{1/2}\}. \tag{3.31}$$

Obviously, there will be no instability occurring in the difference triad interaction.

Equations (3.25) and (3.31) indicate that the triad resonance can only happen in the sum triad interaction (among long, low side-band wave disturbance and the uniform wavetrain) for weakly nonlinear GCW's. Therefore, Hasselmann's criterion [12] is recovered in the case of weakly nonlinear GCW's; and equation (1.1) is only the necessary condition and the first order approximation $O(1/\tilde{T})$ of Hasselmann's criterion in the special case of long and short wave interaction.

In Section 4, accurate computational results will further confirm this conclusion.

4. Numerical results

Accurately solving equation (3.9) serves two purposes. First, the results are used to compare with the results of the strictly numerical method [5]; secondly, the results may confirm the approximate analysis in Section 3, which has shown the characteristics of the triad instability and the recovery of Hasselmann [12] criterion in the case of the deep-water GCW's.

Figures 1 and 2 show the nondimensional linear growth rate of instabilities obtained by (3.9), compared with the results given by strictly numerical computation [5] for $\tilde{T} = 20.0$ and $\tilde{T} = 10.0$ respectively. In Fig. 1(a) ($ka = 0.01$), both results show that the triad instability region and the quartet instability region are not connected, with the quartet instability region located near the origin ($K/k = 0$). Satisfactory comparison is observed in this figure. In Fig. 1(b) ($ka = 0.03$), the triad instability region and the quartet instability region have merged together; both results show this tendency, and the quantitative agreement is good. In Fig. 1(c) ($ka = 0.05$), the differences between the two methods have increased slightly but quantitative agreement is still retained except near $K/k = 0$, where the strictly numerical results show stability. The consistency between the two results is also confirmed in Fig. 2 for $\tilde{T} = 10.0$.

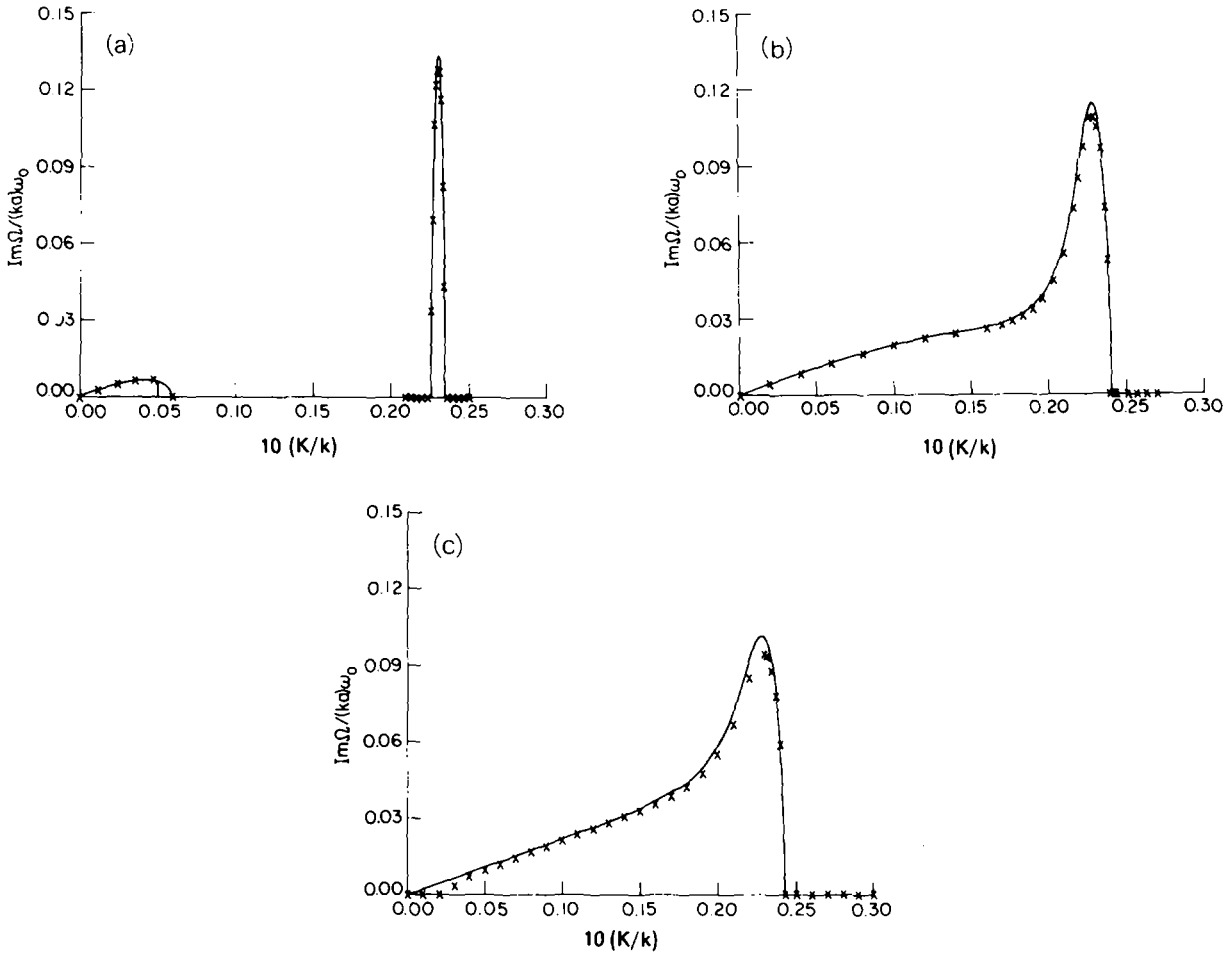

Fig. 1. The linear growth rate of two-dimensional instabilities for $\tilde{T} = 20.0$ derived from the coupled equations (2.19) ——, and the numerical results of Zhang and Melville [5] ×, $ka = 0.01$ (a); $ka = 0.03$ (b); and $ka = 0.05$ (c).

As is observed in Figs. 1 and 2, the bandwidth of the triad instability, normalized by perturbation wave number, is approximately proportional to the wave steepness. For very small wave steepness, say, $ka = 0.01$, the triad instability region is confined to $0.0473 \leq K/k \leq 0{\cdot}0490$, for $\tilde{T} = 10.0$. As shown in Fig. 2(a), the triad instability region is centered at the point where the linear sum triad resonance condition is satisfied; however, the point where the linear difference triad resonance condition is satisfied, and the velocity matching point, are outside of the triad instability region. We may further check the eigenvector corresponding to the eigenvalue whose imaginary part is positive; it is found that the dominant components are $\hat{a}$ and $\hat{b}_2{}^*$, which represent the long wave and the lower side-band disturbances. Hence, it confirms the analytic results that the resonance is due to the sum triad interaction. Typical eigenvectors, for the triad instability, are given in Table 1.

The nondimensional maximum growth rates of the triad instability were obtained by numerically solving (3.9), and are shown in Fig. 3 as a function of the wavesteepness, ka, for various nondimensional surface tension coefficients $\tilde{T}$. For comparison, also shown are the corresponding results by (3.28). Good agreement between the two results is observed for small wave steepness. The above comparison has shown that the

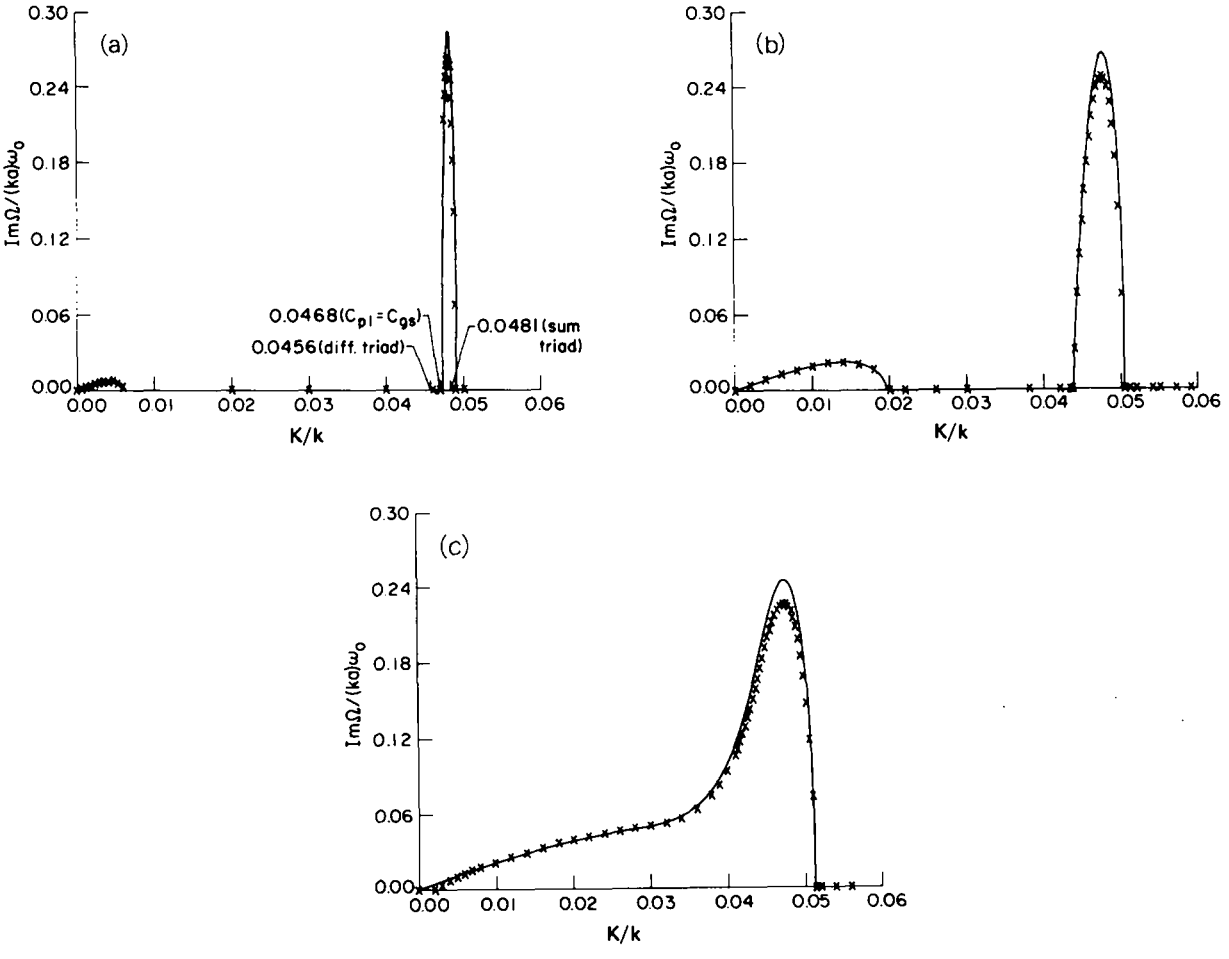

Fig. 2. Same as Fig. 1, except $\tilde{T} = 10.0$.

Table 1
Components of eigenvectors

	Modes	Amplitude[a]
$\tilde{T} = 7.0$, $ka = 0.01$, $K/k = 0.0715$	$\hat{b}_2^*$	1.000
	$\hat{a}$	0.847
	$\hat{b}_1$	0.228
$\tilde{T} = 10.0$, $ka = 0.01$, $K/k = 0.0481$	$\hat{b}_2^*$	1.000
	$\hat{a}$	0.827
	$\hat{b}_1$	0.172
$\tilde{T} = 20.0$, $ka = 0.01$, $K/k = 0.0232$	$\hat{b}_2^*$	1.000
	$\hat{a}$	0.794
	$\hat{b}_1$	0.293

[a] The amplitudes of the disturbance components are normalized such that $\hat{b}_2^* = 1.00$.

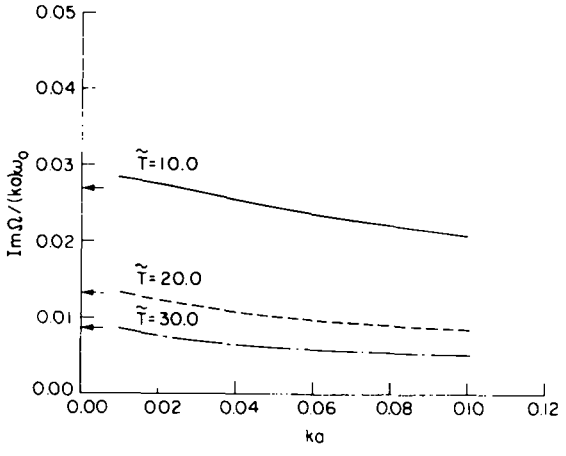

Fig. 3. The maximum growth rates of the triad instability from (3.9) (——, - - - -, — — —, for $\tilde{T} = 10.0, 20.0, 30.0$ respectively), and equation (3.28) (marked by arrows on the vertical axis).

assumption of letting the higher sideband wave be of zero amplitude is reasonable and (3.28) is a good approximation.

Benney [6] showed the linear growth rate of the quartet and triad instabilities in his equations (3.14) and (3.21), respectively. We compared his results[3] with our results for $\tilde{T} = 20.0$ in Fig. 4. When the wave steepness is small, the sum triad instability region is narrow and separated from the quartet instability region; two results are almost coincident as shown in Fig. 4(a). With increasing the steepness, the sum triad instability region begins to connect the quartet instability region; good agreement is still retained around the center of sum triad instability region, whereas large differences are observed at the area where the triad and quartet instability regions have merged, as shown in Figs. 4(b), (c) and (d). The large differences in the region of coalescence are expected, since the rescaled equation [6, eq. (3.21)] is valid only in the immediate neighborhood of the triad resonance ($K/k = 4/9\tilde{T}$) while the area of coalescence is not local.

When the triad and quartet instability regions merge together, the uniform GCW's are unstable to the modulational disturbances whose wave numbers are continuously distributed from very small values up to the value where the triad instability may occur. Yuen and Lake [14] showed that broad-band instabilities may lead to complex wave evolution as a result of the higher harmonics of the fundamental instability also being within the unstable region. We anticipate that similar phenomena may occur for gravity-capillary waves with more complex wave evolution occurring after coalescence, where the most unstable triad instabilities may correspond to harmonics of a quartet instability. It is of interest then to consider dependence of the wave slope at coalescence as a function of $\tilde{T}$. This is shown in Fig. 5, where it may be seen that coalescence occurs at larger ε as $\tilde{T}$ decreases.

The coupled equations (2.19) demonstrate the interaction between long and short waves. They may be used to analyze the stability of the uniform short wave train (GCW's). The validity of the analysis is, however, limited to small values of ε and $1/\tilde{T}$ due to the assumptions made in the derivation of equation (2.19). However, the large $\tilde{T}$ corresponds to wave trains with very short wavelengths, and this may restrict the practical application of the results. First, the strongest triad interaction happens for $\tilde{T}$ slightly larger than 2.[4] Second, waves of very short wavelength are subject to strong viscous dissipation which may

[3] Results based on Benney's theory were computed after the correction of minor algebraic mistakes in his equation (3.21).

[4] With the exception of trivial solutions, the linear sum triad resonance condition is satisfied only for $\tilde{T} \geq 2$.

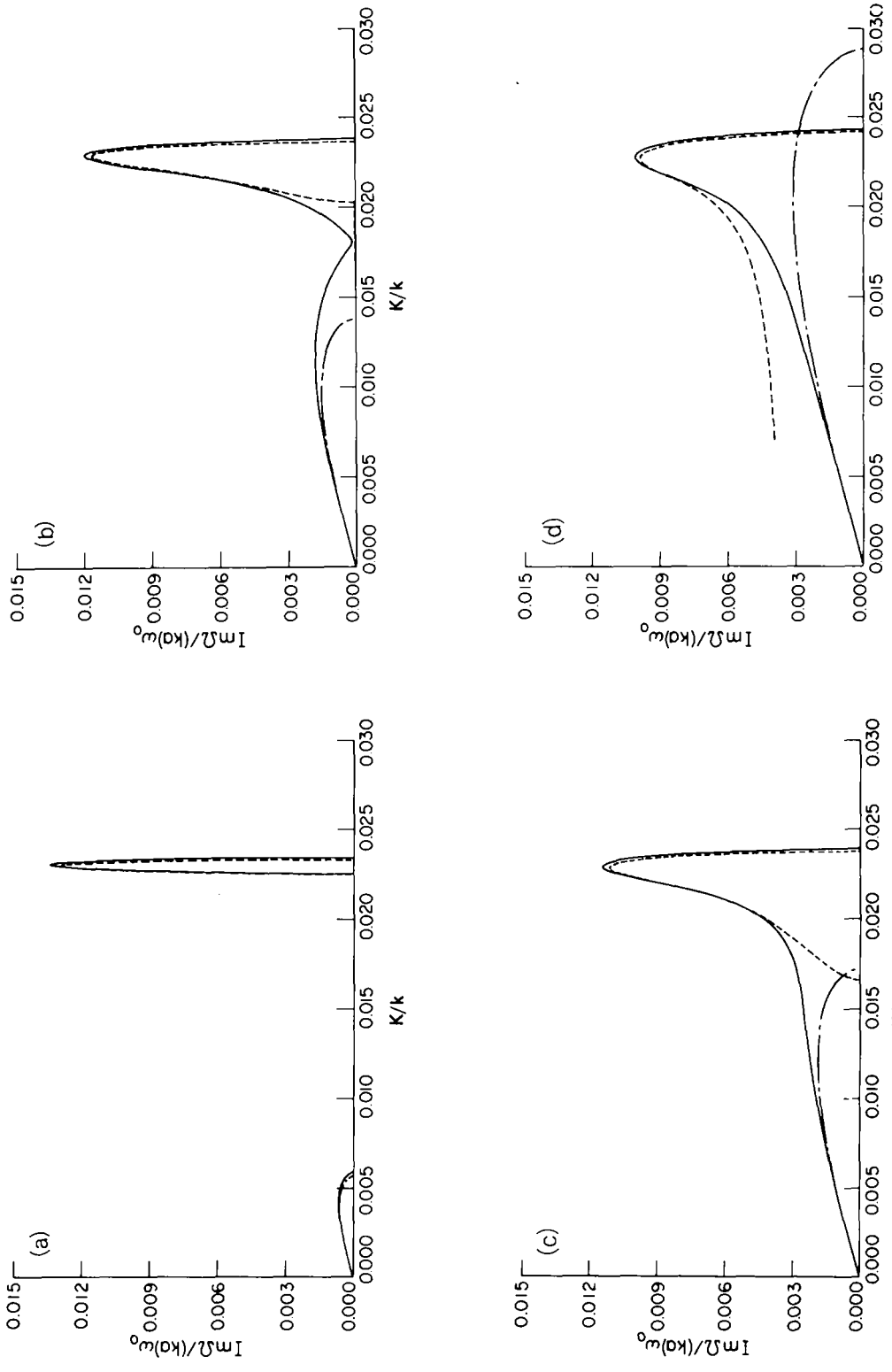

Fig. 4. The linear growth rate of two-dimensional instabilities for $\tilde{T} = 20.0$ derived by equation (3.9) (——), and by Benney [6] (- - - -) [Benney's equation (3.21)] and (— · — · —) [equation (3.14)] for $ka = 0.01$ (a); $ka = 0.024$ (b); $ka = 0.03$ (c); $ka = 0.05$ (d).

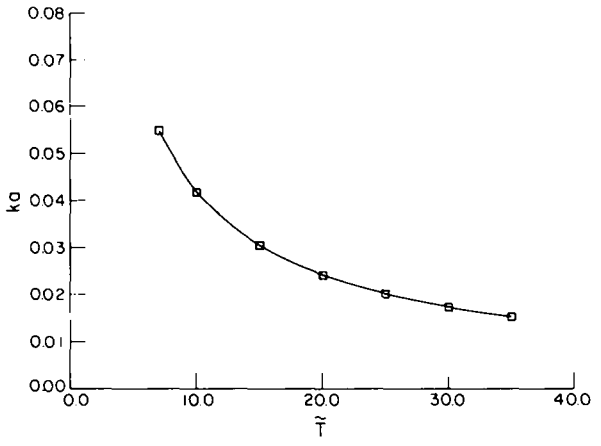

Fig. 5. The wave steepness ka for the onset of coalescence of the triad and quartet instability regions, shown as a function of $\tilde{T}$.

dominate nonlinear effects, with the result that the triad resonant interactions may not be observed. Therefore, full numerical methods are necessary to extend the study into parametric ranges of more practical interest as has been done in [5].

Acknowledgment

We wish to thank Professor C.C. Mei for helpful discussions of preliminary results of this research. This work was supported by the National Science Foundation through grants MEA 82-10649 and OCE-8214746.

Appendix A

In Section 2, we have the following equations:

$$l_c = \mu\left(\frac{T}{\rho g}\right)^{1/2}, \qquad t_c = \mu\left(\frac{l_c}{l_g}\right)^{1/2}. \tag{2.7}$$

Let the subscript d denote the dimensional variable. From $\exp(ixk) = \exp(ix_d k/l_c) = \exp(ix_d k_d)$, we have

$$k = l_c k_d. \tag{A.1}$$

Similarly,

$$K = K_d l_c, \qquad \omega = t_c \omega_d, \qquad \Omega = t_c \Omega_d. \tag{A.2,3,4}$$

From (A.2)-(A.4), we notice

$$K/k = K_d/k_d, \qquad \Omega/\omega = \Omega_d/\omega_d. \tag{A.5}$$

Using (2.7), (A.1) may be written as

$$k = k_d l_c = \mu\left(\frac{k_d^2 T}{\rho g}\right)^{1/2} = \mu \tilde{T}^{1/2},$$

where

$$\tilde{T} = \frac{k_d^2 T}{\rho g}, \tag{A.6}$$

is the nondimensional surface tension coefficient. Therefore

$$\mu^2 = k^2/\tilde{T}. \tag{A.7}$$

Using (A.7), we obtain

$$\varepsilon\lambda/k^2 = \mu^2/k^2 = 1/\tilde{T}. \tag{3.8}$$

In Section 2, we have

$$\eta_d = \eta_c \eta, \qquad \eta_c/l_c = \varepsilon, \tag{2.6, 2.8}$$

where η is the nondimensional amplitude of the wave train. Therefore

$$\eta = \frac{\eta_d}{\eta_c} = \frac{\eta_d k_d}{\eta_c k_d} = \frac{\eta_d k_d}{k\eta_c/l_c} = \frac{\varepsilon'}{k\varepsilon},$$

where $\varepsilon' = \eta_d k_d$, the wave slope of the wave train.

Taking

$$\varepsilon' = \varepsilon, \tag{A.8}$$

that is the nondimensional wave slope is the same as the real wave slope, we have

$$\eta = 1/k. \tag{A.9}$$

From (2.16), $\eta \tilde{=} \eta^{(11)} e^{i\theta} + *$; therefore, $|\eta|_{max} \cong 2|\eta^{(11)}|$. Also from (2.20), (2.21) and (3.4),

$$|\eta^{(11)}| = \frac{k}{\omega}|B| = \frac{k^2}{\omega^2}|S_0| = \frac{1}{k}|S_0|,$$

hence,

$$|S_0| = \tfrac{1}{2}. \tag{3.7}$$

Appendix B

Neglecting higher order $O(\varepsilon^2)$ error, eqs. (2.19a) and (2.19b) may be combined to give

$$\phi^{(0)}_{t_1 t_1} + \lambda\phi^{(0)}_{z_1} = 2\frac{\varepsilon\lambda\omega}{k}(BB^*)_{x_1} - \frac{\varepsilon}{\lambda}\phi^{(0)}_{t_1 t_1 x_1 x_1}. \tag{B.1}$$

Substituting (3.2), (3.4) into (B.1), using (3.7) and (3.8), eq. (B.1) may be reduced to

$$\left(\frac{\Omega}{\omega}\right)^2 - \frac{1}{\tilde{T}}\left(\frac{K}{k}\right) = O\left[\frac{\varepsilon}{\tilde{T}^2}, \frac{1}{\tilde{T}^3}\right]. \tag{B.2}$$

Using (B.2), we have

$$\frac{1}{\tilde{T}}\frac{[1+\tilde{T}(K/k)^2]}{\Omega/\omega} = \frac{\Omega/\omega[1+\tilde{T}(K/k)^2]}{K/k} + O\left[\frac{\varepsilon}{\tilde{T}^2}, \frac{1}{\tilde{T}^3}\right] = \frac{\Omega/K}{\omega/k} + O\left[\varepsilon, \frac{1}{\tilde{T}}\right].$$

Notice, $C_{PL} = \Omega/K$ and $C_{PS} = k/\omega$, whence

$$\frac{1}{\tilde{T}} \frac{[1+\tilde{T}(K/k)^2]}{\Omega/\omega} = \frac{C_{PL}}{C_{PS}} + O\left(\frac{1}{\tilde{T}}, \varepsilon\right). \tag{3.13}$$

We have assumed

$$\frac{K}{k} = \frac{4}{9\tilde{T}}(1+\varepsilon K_r), \quad K_r \sim O(1), \tag{3.19}$$

$$\frac{\Omega}{\omega} = \frac{2}{3\tilde{T}}\left(1-\frac{1}{6\tilde{T}}\right)(1+\varepsilon K_r)(1+\Omega_r). \tag{3.20}$$

Substituting (3.19) and (3.20) into (B.2), we have

$$\Omega_r = O(\varepsilon, 1/\tilde{T}). \tag{3.21a}$$

References

[1] M.S. Longuet-Higgins, "The instabilities of gravity waves of finite amplitude in deep water. I. Superharmonics", *Proc. Roy. Soc. London Ser. A 360*, 471-488 (1978).

[2] M.S. Longuet-Higgins, "The instabilities of gravity waves of finite amplitude in deep water. II. Subharmonics", *Proc. Roy. Soc. London Ser. A 360*, 489-505 (1978).

[3] J.W. McLean, Y.C. Ma, D.U. Martin, P.G. Saffman and H.C. Yuen, "A new type of three-dimensional instability of finite amplitude gravity waves", *Phys. Rev. Letters 46* (13), 817-820 (1981).

[4] J.W. McLean, "Instabilities of finite-amplitude water waves", *J. Fluid Mech. 114*, 315-330 (1982).

[5] J. Zhang and W.K. Melville, "Three dimensional instabilities of nonlinear gravity-capillary waves", *J. Fluid Mech.* (1986), to appear.

[6] D.J. Benney, "Significant interactions between small and large scale surface waves", *Studies Appl. Math. 55*, 93-105 (1976).

[7] D.J. Djordjevic and L.G. Redekopp, "On two-dimensional packets of capillary-gravity waves", *J. Fluid Mech. 79*, 703-714 (1977).

[8] D.J. Benney, "A general theory for interactions between short and long waves", *Studies Appl. Math. 56*, 81-94 (1977).

[9] Y.C. Ma, "The complete solution of the long-wave-short-wave resonance equations", *Studies Appl. Math. 59*, 202-221 (1978).

[10] Y.C. Ma and L.G. Redekopp, "Some solutions pertaining to the resonant interaction of long and short waves", *Phys. Fluids 22*, 1872-1876 (1979).

[11] Y.C. Ma, "A note on the instability of capillary waves", Personal communication, 1981.

[12] K. Hasselmann, "A criterion for nonlinear wave stability", *J. Fluid Mech. 30*, 737-739 (1967).

[13] Reference Manual, IMSL Library, edition 8, 1980.

[14] H.C. Yuen and B.M. Lake, "Nonlinear dynamics of deep-water gravity waves", *Adv. Appl. Mech. 22*, 67-229 (1982).